Changes in behavioral state account for the modulation of cerebellar learning by cannabinoid receptors

*Catarina Albergaria, N. Tatiana Silva, Dana Darmohray, Megan R. Carey**
Champalimaud Neuroscience Program, Champalimaud Center for the Unknown, Lisbon, Portugal

* Correspondence:

Megan R. Carey
email: megan.carey@neuro.fchampalimaud.org
twitter: @meganinlisbon

Abstract

Attempts to identify cellular mechanisms underlying learning often include knocking out genes involved in candidate forms of synaptic plasticity and assessing subsequent effects on behavior. Within the cerebellum, multiple plasticity mechanisms have been proposed as cellular substrates of learning. For example, type 1-cannabinoid receptors (CB1Rs) mediate several forms of synaptic plasticity in the cerebellar cortex and have been implicated in cerebellum-dependent delay eyeblink conditioning in knockout experiments. However, recent work has shown that eyeblink conditioning is modulated by behavioral state, and global CB1KO mice are known to be hypoactive. We therefore asked to what extent altered locomotor activity vs. impaired CB1-dependent plasticity within the cerebellar cortex contribute to learning impairments in these mice. We find that eyeblink conditioning deficits in global CB1KOs can be fully accounted for by their hypoactivity. Impairments disappear when the level of locomotor activity is taken into account, and externally controlling running speed rescues learning. Moreover, both global and cerebellar granule cell-specific CB1KOs exhibit normal cerebellum-dependent locomotor adaptation. Our results suggest that the apparent effects of CB1R deletion on cerebellar learning are not due to direct effects on CB1-dependent plasticity, but rather, arise as a secondary consequence of hypoactivity. These findings highlight the importance of considering general changes in behavioral state as a powerful means through which individual genes contribute to complex behaviors, particularly in transgenic models.

Introduction

Knockout animals have been used extensively to investigate the role of specific receptors and signaling pathways in complex behaviors such as learning and memory (Crawley, 2008; Dubnau and Tully, 1998; Picciotto and Wickman, 1998). The sometimes conflicting findings from this approach are often attributed to its widely-acknowledged drawbacks, including limited cellular and temporal specificity (El-Brolosy and Stainier, 2017). Possible compensatory effects of chronic gene deletion, as well as both the level of cell-type specificity and multiple signaling targets within cells, all need to be taken into consideration.

The cerebellum has been used extensively as a model system for linking cellular plasticity and learning. Simple forms of learning, such as delay eyeblink conditioning, in which animals learn to close their eye in response to a neutral conditioned stimulus (CS) that is consistently paired with an puff of air to the eye, are known to take place within the cerebellum (Heiney et al., 2014; McCormick and Thompson, 1984). The well-described cerebellar circuit architecture places strong constraints on the sites and mechanisms for learning. Despite these advantages, however, results from gene knockout studies have contributed to controversies about how specific plasticity mechanisms, including long-term depression between parallel fibers (the axons of granule cells) and Purkinje cells, contribute to cerebellar learning (Ito, 1972; Aiba et al., 1994; Carey, 2011; De Zeeuw et al., 1998; Koekkoek et al., 2003; Schonewille et al., 2011).

Endocannabinoids, retrograde messengers that act via type-1 cannabinoid receptors (CB1Rs) to mediate short- and long-term forms of synaptic plasticity throughout the brain (Chevaleyre et al., 2006; Freund et al., 2003; Kreitzer and Regehr, 2002; Regehr et al., 2009), have been implicated in several forms of plasticity within the cerebellar cortex (Brenowitz and Regehr, 2005; Brown et al., 2003; Kreitzer and Regehr, 2001a, 2001b; Soler-Llavina and Sabatini, 2006), including parallel fiber LTD (Safo and Regehr, 2005; Carey et al., 2011). A previous study (Kishimoto and Kano, 2006) found that global CB1 knockout (CB1KO) mice were impaired in delay eyeblink conditioning, suggesting that this deficit in cerebellar learning could be due to deficient parallel fiber LTD. However, this has not been directly tested.

Mutant mice lacking CB1 receptors display a variety of additional behavioral phenotypes. Notably, global CB1KOs are hypoactive, and spend less time running than their wildtype littermates (Chaouloff et al., 2011; Dubreucq et al., 2010; Zimmer et al., 1999). This hypoactivity has been attributed to the loss of CB1Rs from GABAergic neurons in the ventral tegmental area (Dubreucq et al., 2013). They also exhibit altered levels of anxiety and impaired spatial memory and extinction of fear conditioning (Degroot and Nomikos, 2004; Marsicano et al., 2002; Pamplona and Takahashi, 2006; Varvel and Lichtman, 2002).

We recently demonstrated that engaging in locomotor activity modulates learning of delay eyeblink conditioning (Albergaria et al., 2018). This raises the possibility that the hypoactivity of CB1KO mice could indirectly contribute to their apparent impairments in learning for this task. Here we investigate the relative contributions of decreased locomotor activity vs. altered CB1R-dependent synaptic plasticity to cerebellum-dependent learning in global and cell-type specific CB1KO mice. We conclude that the previously described effects of CB1R deletion on cerebellum-dependent learning arise as a secondary consequence of hypoactivity in CB1KOs, and not from direct effects on cerebellar plasticity. These findings highlight the importance of considering general changes in behavioral state as a potential mechanism through which individual genes contribute to complex behaviors in transgenic models.

Results

CB1KOs are hypoactive and have apparent delays in eyeblink conditioning

We tested cerebellum-dependent delay eyeblink conditioning in global CB1KO mice and their wildtype littermates using a head-fixed apparatus with a freely rotating running wheel (Fig. 1A, B), as previously described (Albergaria et al., 2018; Chettih et al., 2011). Conditioning sessions included 100 trials in which a neutral visual conditioned stimulus (CS, a white LED) was paired with an air-puff unconditioned stimulus (US; a 50ms, 40psi air-puff directed at the eye). The CS preceded the US by 300ms and the two stimuli co-terminated. We measured the mouse's locomotor activity continuously with an infrared sensor placed underneath the wheel (Fig. 1A).

Consistent with a previous study that found impaired learning over seven acquisition sessions (Kishimoto and Kano, 2006), we found that CB1KOs displayed delayed learning, as measured by the percentage of trials that yielded a learned conditioned responses (CR; Fig. 1C). When compared to their littermate controls, CB1KO mice displayed significantly less locomotor activity on the self-paced running wheel during training sessions (Fig. 1D, $p < 0.05$), consistent with the previously described hypoactivity of these mice (Chaouloff et al., 2011; Dubreucq et al., 2010; Zimmer et al., 1999).

Because of the recently described modulation of eyeblink conditioning by locomotor activity (Albergaria et al., 2018; Chettih et al., 2011), we asked whether the hypoactivity of CB1KOs could contribute to their delayed learning. We found that regardless of genotype, the more an animal ran on average, the earlier it learned (Fig. 1E; controls: slope=-44.2, $p < 0.05$; CB1KO: slope = -66.5, $p < 0.05$). Over the course of 20 training sessions, however, we found that both genotypes eventually learned the task (Fig. 1F). Comparing acquisition curves of CB1KOs with littermate controls with comparable activity levels (Fig. 1F, thick red and black lines) revealed no delays in learning in the CB1KOs, suggesting that locomotor activity is a stronger determinant of rate of learning than is genotype.

Trial-to-trial CR amplitudes are modulated by locomotor activity in CB1KOs

The amplitude and timing of conditioned responses were generally normal in CB1KOs (Fig. 1G-I). As previously described in wildtype mice (Albergaria et al., 2018), trial-to-trial variation in the amplitude of conditioned responses was positively correlated with locomotor speed in both global CB1KOs and their littermate controls (Fig. 1G,H; CB1KO: n=2470 trials, N=11 animals, $F_{(1,45.5)} = 62.4$, $p < 0.0001$; littermate controls: n=2639 trials, N=12 animals, $F_{(1,73.7)} = 35.9$, $p < 0.0001$) (Fig. 1H). Interestingly, there was a tendency for CB1KOs to have *larger* CR amplitudes when compared to speed-matched trials from control mice (Fig. 1H; $F_{(1,41.03)} = 26.4$, $p < 0.0001$). This surprising result likely accounts for the finding (Fig. 1I) that overall, the average CR amplitudes for the two genotypes were not significantly different, despite the slower speed distributions in CB1KOs (histograms in Fig. 1H).

Externally controlling locomotor speed rescues learning deficits in CB1KOs

If the delayed eyeblink conditioning observed in CB1KOs is a consequence of their hypoactivity, then circumventing it by externally controlling running speed (Albergaria et al., 2018) should be sufficient to rescue learning. Indeed, replacing the self-paced running wheel with a motorized treadmill that equalized locomotor activity across mice completely eliminated the delayed learning of CB1KOs (Fig. 2A, B). The average amplitude of eyelid responses was also not statistically different between the two genotypes under these conditions (Fig. 2C, D). Interestingly, in line with the results of Fig. 1H, when running speed was fixed, there was a trend for CB1KOs to learn faster (Fig. 2A, B) and to have larger CR amplitudes (Fig. 2C, D) when compared to littermate controls.

Parallel fiber CB1 receptors are not required for delay eyeblink conditioning

The impaired eyeblink conditioning in global CB1KOs has been hypothesized (Carey et al., 2011; Kishimoto and Kano, 2006) to be due to the loss of CB1Rs from parallel fibers, where they mediate several forms of synaptic plasticity, including parallel fiber LTD (Brenowitz and Regehr, 2005; Carey et al., 2011; Kreitzer and Regehr, 2001a, 2001b; Safo and Regehr, 2005; Soler-Llavina and Sabatini, 2006). In contrast, our results so far suggest that the apparent effects of CB1R deletion on eyeblink conditioning may arise as a secondary consequence of the hypoactivity of global CB1KOs. However, they do not necessarily rule out a possible additional role for parallel fiber CB1Rs in eyeblink conditioning. To address this, we tested eyeblink conditioning in mice in which CB1Rs were selectively deleted from cerebellar granule cells (g6CB1KO, Fig. 3B), whose axons form parallel fibers (Carey et al., 2011; Fünfschilling and Reichardt, 2002).

Consistent with an extracerebellar source of decreased locomotor activity in global CB1KOs (Dubreucq et al., 2013), g6CB1KO mice were not hypoactive (Fig. 3C). Further, delay eyeblink conditioning was intact in granule-cell specific CB1 knockout mice compared to littermate controls (Fig. 3A). Unlike global CB1KOs, neither the distribution of running speeds nor the speed-matched CR amplitudes differed between g6CB1KOs and controls (Fig. 3D). There was also no difference in learning between the two groups on a motorized treadmill (Fig. 3E-G).

Taken together, these results suggest that none of the differences in eyeblink conditioning in global CB1KO mice are due to the loss of CB1Rs from cerebellar parallel fibers.

CB1Rs are dispensable for locomotor learning

There are many similarities between learning mechanisms for eyeblink conditioning and other forms of cerebellum-dependent learning such as motor adaptation (Raymond et al., 1996). However, there are also important differences, particularly in the time course of learning, which could be particularly relevant in the context of CB1-mediated plasticity, which often acts on shorter time scales. We therefore investigated whether CB1Rs might play a role in locomotor adaptation on a split-belt treadmill, which is another form of cerebellum-dependent learning (Morton and Bastian 1996; Yanagihara et al. 1996; Darmohray et al., 2018). This also provided an opportunity to analyze the gait of CB1KO mice for any potential signs of cerebellar ataxia (Supp. Fig. 1B).

In locomotor adaptation on a split-belt treadmill, animals learn to regain overall gait symmetry in response to a perturbation that imposes unequal speeds on the two sides of the body (Fig. 4A). Learning is specific to measures of interlimb coordination, such as step-length (Fig. 4B, see Methods); whereas individual limb parameters, such as stride-length (Fig. 4B), change with the changes in belt speed but do not show learning (Reisman et al., 2005; Darmohray et al., 2018).

Global CB1KO mice were not visibly ataxic, and on the split-belt treadmill, they adjusted their stride lengths appropriately to match belt speeds (Fig. 4C, $t_{(14)} = -0.36$, $p = 0.73$). Detailed gait analysis revealed some mild gait differences that did not fit the pattern of cerebellar ataxia (Supp. Fig. 1B) (Machado et al., 2015). Despite smaller initial errors in step-length upon the onset of split-belt walking, CB1KOs successfully regained interlimb symmetry during split-belt walking (Fig. 4D). Learning, as measured by step-length aftereffect (Darmohray et al., 2018) was intact (Fig. 4D).

Finally, both locomotion and locomotor learning were indistinguishable from controls in granule cell-specific CB1KOs, who exhibited none of the gait alterations observed in global knockouts (Fig. 4E,F).

Thus, both global and cell-type specific CB1KO mice show normal cerebellum-dependent locomotor learning.

Discussion

Several lines of evidence presented here support the conclusion that the apparent effects of global CB1R deletion on cerebellar learning arise as a secondary consequence of the hypoactivity of global CB1KOs, rather than through direct effects on cerebellar plasticity. First, the delayed eyeblink conditioning in global CB1KOs was fully accounted for by differences in locomotor activity across animals (Fig. 1E,F). Second, learning impairments of CB1KO mice were rescued by externally controlling running speed. In fact, under conditions with comparable levels of locomotor activity, global CB1KOs exhibited improved performance relative to controls (e.g. Fig. 1F,H, Fig. 2). Third, global CB1KOs did not show signs of cerebellar ataxia (Supp. Fig. 1), and cerebellum-dependent locomotor learning was normal in these mice (Fig. 4E,F). Finally, granule cell-specific CB1KO mice exhibited none of the behavioral phenotypes observed in global knockouts (Figs. 3,4), suggesting that they do not depend on CB1Rs in parallel fibers.

Our findings suggest that parallel fiber CB1Rs are dispensable for cerebellum-dependent learning, but they do not rule out a possible role for LTD. While previous studies have demonstrated a role for CB1Rs in parallel fiber LTD (Carey et al., 2011; Safo and Regehr, 2005), this form of plasticity has been investigated *in vitro* with several different induction protocols (for review see Carey, 2011; Hansel et al., 2001). It is not known which of the resulting plasticity mechanisms are invoked *in vivo* during behavioral learning, and it is possible that not all forms of LTD are CB1-dependent. Moreover, there could be compensatory mechanisms in the knockouts that mask the behavioral consequences of the loss of CB1R-dependent LTD.

We show here that despite the strong constraints placed on the sites and mechanisms for delay eyeblink conditioning, CB1R deletion modulates this form of cerebellum-dependent learning via indirect, extracerebellar (Dubreucq et al., 2013) effects on behavioral state. By demonstrating that controlling locomotor activity levels can rescue apparent learning deficits in mutant mice, the current findings extend recent work showing that behavioral state is a powerful modulator of brain function (Ayaz et al., 2013; Bennett et al., 2013; Dadarlat and Stryker, 2017; Dipoppa et al., 2018; Erisken et al., 2014; Niell and Stryker, 2010; Pinto et al., 2013; Polack et al., 2013; Musall et al., 2018; Vinck et al., 2015), including capacity for learning (Albergaria et al., 2018). Further, they draw attention to the importance of considering altered levels of locomotor activity as an additional potential confound in gene knockout studies (Crawley, 2008; Eisener-Dorman et al., 2009; El-Brolosy and Stainier, 2017; Picciotto and Wickman, 1998).

Acknowledgements

We thank Tracy Pritchett and Ana Vaz for maintenance of mouse lines. We thank Wade Regehr and Rui Costa for helpful discussions and support during the initial planning of this project. We are grateful to the members of Carey lab and the Champalimaud Neuroscience Program for helpful discussion.

This work was supported by a Howard Hughes Medical Institute International Early Career Scientist Grant #55007413 (to MRC), a European Research Council Starting Grant #640093 (to MRC), Bial Foundation Research Bursary #74/14, and fellowships from the Portuguese Fundação para a Ciência e a Tecnologia SFRH/BD/77686/2011 (to CA), SFRH/BD/105949/2014 (to NTS), SFRH/BD/86265/2012 (to DD).

References

Aiba, A., Kano, M., Chen, C., Stanton, M.E., Fox, G.D., Herrup, K., Zwingman, T.A., and Tonegawa, S. (1994). Deficient cerebellar long-term depression and impaired motor learning in mGluR1 mutant mice. Cell *79*, 377–388.

Albergaria, C., Silva, N.T., Pritchett, D.L., and Carey, M.R. (2018). Locomotor activity modulates associative learning in mouse cerebellum. Nat. Neurosci. *21*, 725–735.

Albus, J.S. (1971). A theory of cerebellar function. Math. Biosci. *10*, 25–61.

Ayaz, A., Saleem, A.B., Schölvinck, M.L., and Carandini, M. (2013). Locomotion controls spatial integration in mouse visual cortex. Curr. Biol. *23*, 890–894.

Bennett, C., Arroyo, S., and Hestrin, S. (2013). Subthreshold mechanisms underlying state-dependent modulation of visual responses. Neuron *80*, 350–357.

Brenowitz, S.D., and Regehr, W.G. (2005). Associative short-term synaptic plasticity mediated by endocannabinoids. Neuron *45*, 419–431.

Brown, S.P., Brenowitz, S.D., and Regehr, W.G. (2003). Brief presynaptic bursts evoke synapse-specific retrograde inhibition mediated by endogenous cannabinoids. Nat. Neurosci. *6*, 1048–1057.

Carey, M.R. (2011). Synaptic mechanisms of sensorimotor learning in the cerebellum. Curr. Opin. Neurobiol. *21*, 609–615.

Carey, M.R., Myoga, M.H., McDaniels, K.R., Marsicano, G., Lutz, B., Mackie, K., and Regehr, W.G. (2011). Presynaptic CB1 receptors regulate synaptic plasticity at cerebellar parallel fiber synapses. J. Neurophysiol. *105*, 958–963.

Chaouloff, F., Dubreucq, S., Bellocchio, L., and Marsicano, G. (2011). Endocannabinoids and motor behavior: CB1 receptors also control running activity. Physiology *26*, 76–77; author reply 78.

Chettih, S.N., McDougle, S.D., Ruffolo, L.I., and Medina, J.F. (2011). Adaptive timing of motor output in the mouse: the role of movement oscillations in eyelid conditioning. Front. Integr. Neurosci. *5*, 72.

Chevaleyre, V., Takahashi, K.A., and Castillo, P.E. (2006). Endocannabinoid-mediated synaptic plasticity in the CNS. Annu. Rev. Neurosci. *29*, 37–76.

Crawley, J.N. (2008). Behavioral phenotyping strategies for mutant mice. Neuron *57*, 809–818.

Dadarlat, M.C., and Stryker, M.P. (2017). Locomotion Enhances Neural Encoding of Visual Stimuli in Mouse V1. J. Neurosci. *37*, 3764–3775.

Darmohray, D., Jacobs, J., Marques, H.G., and Carey, M.R. (2018). Spatial and temporal locomotor learning in mouse cerebellum. bioRxiv.

Degroot, A., and Nomikos, G.G. (2004). Genetic deletion and pharmacological blockade of CB1 receptors modulates anxiety in the shock-probe burying test. Eur. J. Neurosci. *20*, 1059–1064.

De Zeeuw, C.I., Hansel, C., Bian, F., Koekkoek, S.K., van Alphen, A.M., Linden, D.J., and Oberdick, J. (1998). Expression of a protein kinase C inhibitor in Purkinje cells blocks cerebellar LTD and adaptation of the vestibulo-ocular reflex. Neuron *20*, 495–508.

Dipoppa, M., Ranson, A., Krumin, M., Pachitariu, M., Carandini, M., and Harris, K.D. (2018). Vision and Locomotion Shape the Interactions between Neuron Types in Mouse Visual Cortex. Neuron *98*, 602–615.e8.

Dubnau, J., and Tully, T. (1998). Gene discovery in Drosophila: new insights for learning and memory. Annu. Rev. Neurosci. *21*, 407–444.

Dubreucq, S., Koehl, M., Abrous, D.N., Marsicano, G., and Chaouloff, F. (2010). CB1 receptor deficiency decreases wheel-running activity: consequences on emotional behaviours and hippocampal neurogenesis. Exp. Neurol. *224*, 106–113.

Dubreucq, S., Durand, A., Matias, I., Bénard, G., Richard, E., Soria-Gomez, E., Glangetas, C., Groc, L., Wadleigh, A., Massa, F., et al. (2013). Ventral tegmental area cannabinoid type-1 receptors control voluntary exercise performance. Biol. Psychiatry *73*, 895–903.

Eisener-Dorman, A.F., Lawrence, D.A., and Bolivar, V.J. (2009). Cautionary insights on knockout mouse studies: the gene or not the gene? Brain Behav. Immun. *23*, 318–324.

El-Brolosy, M.A., and Stainier, D.Y.R. (2017). Genetic compensation: A phenomenon in search of

mechanisms. PLoS Genet. *13*, e1006780.

Erisken, S., Vaiceliunaite, A., Jurjut, O., Fiorini, M., Katzner, S., and Busse, L. (2014). Effects of locomotion extend throughout the mouse early visual system. Curr. Biol. *24*, 2899–2907.

Freund, T.F., Katona, I., and Piomelli, D. (2003). Role of endogenous cannabinoids in synaptic signaling. Physiol. Rev. *83*, 1017–1066.

Fünfschilling, U., and Reichardt, L.F. (2002). Cre-mediated recombination in rhombic lip derivatives. Genesis *33*, 160–169.

Hansel, C., Linden, D.J., and D'Angelo, E. (2001). Beyond parallel fiber LTD: the diversity of synaptic and non-synaptic plasticity in the cerebellum. Nat. Neurosci. *4*, 467–475.

Heiney, S.A., Wohl, M.P., Chettih, S.N., Ruffolo, L.I., and Medina, J.F. (2014). Cerebellar-dependent expression of motor learning during eyeblink conditioning in head-fixed mice. Journal of Neuroscience *34*, 14845–14853.

Ito, M. (1972). Neural design of the cerebellar motor control system. Brain Res. *40*, 81–84.

Kishimoto, Y., and Kano, M. (2006). Endogenous cannabinoid signaling through the CB1 receptor is essential for cerebellum-dependent discrete motor learning. J. Neurosci. *26*, 8829–8837.

Koekkoek, S.K.E., Hulscher, H.C., Dortland, B.R., Hensbroek, R.A., Elgersma, Y., Ruigrok, T.J.H., and De Zeeuw, C.I. (2003). Cerebellar LTD and learning-dependent timing of conditioned eyelid responses. Science *301*, 1736–1739.

Kreitzer, A.C., and Regehr, W.G. (2001a). Cerebellar depolarization-induced suppression of inhibition is mediated by endogenous cannabinoids. J. Neurosci. *21*, RC174.

Kreitzer, A.C., and Regehr, W.G. (2001b). Retrograde inhibition of presynaptic calcium influx by endogenous cannabinoids at excitatory synapses onto Purkinje cells. Neuron *29*, 717–727.

Kreitzer, A.C., and Regehr, W.G. (2002). Retrograde signaling by endocannabinoids. Curr. Opin. Neurobiol. *12*, 324–330.

Lalonde, R., and Strazielle, C. (2007). Spontaneous and induced mouse mutations with cerebellar dysfunctions: behavior and neurochemistry. Brain Res. *1140*, 51–74.

Machado, A.S., Darmohray, D.M., Fayad, J., Marques, H.G., and Carey, M.R. (2015). A quantitative framework for whole-body coordination reveals specific deficits in freely walking ataxic mice. Elife *4*.

Mariani, J., Crepel, F., Mikoshiba, K., Changeux, J.P., and Sotelo, C. (1977). Anatomical, physiological and biochemical studies of the cerebellum from Reeler mutant mouse. Philos. Trans. R. Soc. Lond. B Biol. Sci. *281*, 1–28.

Marsicano, G., Wotjak, C.T., Azad, S.C., Bisogno, T., Rammes, G., Cascio, M.G., Hermann, H., Tang, J., Hofmann, C., Zieglgänsberger, W., et al. (2002). The endogenous cannabinoid system controls extinction of aversive memories. Nature *418*, 530–534.

Marsicano, G., Goodenough, S., Monory, K., Hermann, H., Eder, M., Cannich, A., Azad, S.C., Cascio, M.G., Gutiérrez, S.O., van der Stelt, M., et al. (2003). CB1 cannabinoid receptors and on-demand defense against excitotoxicity. Science *302*, 84–88.

McCormick, D.A., and Thompson, R.F. (1984). Cerebellum: essential involvement in the classically conditioned eyelid response. Science *223*, 296–299.

Morton, S.M. (2006a). Cerebellar Contributions to Locomotor Adaptations during Splitbelt Treadmill Walking. J. Neurosci. *26*, 9107–9116.

Mullen, R.J., Eicher, E.M., and Sidman, R.L. (1976). Purkinje cell degeneration, a new neurological mutation in the mouse. Proc. Natl. Acad. Sci. U. S. A. *73*, 208–212.

Musall, S., Kaufman, M.T., Gluf, S., and Churchland, A.K. (2018). Movement-related activity dominates cortex during sensory-guided decision making. bioRxiv.

Niell, C.M., and Stryker, M.P. (2010). Modulation of visual responses by behavioral state in mouse visual cortex. Neuron *65*, 472–479.

Pamplona, F.A., and Takahashi, R.N. (2006). WIN 55212-2 impairs contextual fear conditioning through the activation of CB1 cannabinoid receptors. Neurosci. Lett. *397*, 88–92.

Picciotto, M.R., and Wickman, K. (1998). Using knockout and transgenic mice to study

neurophysiology and behavior. Physiol. Rev. *78*, 1131–1163.

Pinto, L., Goard, M.J., Estandian, D., Xu, M., Kwan, A.C., Lee, S.-H., Harrison, T.C., Feng, G., and Dan, Y. (2013). Fast modulation of visual perception by basal forebrain cholinergic neurons. Nat. Neurosci. *16*, 1857–1863.

Polack, P.-O., Friedman, J., and Golshani, P. (2013). Cellular mechanisms of brain state-dependent gain modulation in visual cortex. Nat. Neurosci. *16*, 1331–1339.

Raymond, J.L., Lisberger, S.G., and Mauk, M.D. (1996). The cerebellum: a neuronal learning machine? Science *272*, 1126–1131.

Regehr, W.G., Carey, M.R., and Best, A.R. (2009). Activity-dependent regulation of synapses by retrograde messengers. Neuron *63*, 154–170.

Reisman, D.S., Block, H.J., and Bastian, A.J. (2005). Interlimb coordination during locomotion: what can be adapted and stored? J. Neurophysiol. *94*, 2403–2415.

Safo, P.K., and Regehr, W.G. (2005). Endocannabinoids control the induction of cerebellar LTD. Neuron *48*, 647–659.

Schonewille, M., Gao, Z., Boele, H.-J., Veloz, M.F.V., Amerika, W.E., Simek, A.A.M., De Jeu, M.T., Steinberg, J.P., Takamiya, K., Hoebeek, F.E., et al. (2011). Reevaluating the role of LTD in cerebellar motor learning. Neuron *70*, 43–50.

Soler-Llavina, G.J., and Sabatini, B.L. (2006). Synapse-specific plasticity and compartmentalized signaling in cerebellar stellate cells. Nat. Neurosci. *9*, 798–806.

Varvel, S.A., and Lichtman, A.H. (2002). Evaluation of CB1 receptor knockout mice in the Morris water maze. J. Pharmacol. Exp. Ther. *301*, 915–924.

Vinck, M., Batista-Brito, R., Knoblich, U., and Cardin, J.A. (2015). Arousal and locomotion make distinct contributions to cortical activity patterns and visual encoding. Neuron *86*, 740–754.

Yanagihara, D., and Kondo, I. (1996). Nitric oxide plays a key role in adaptive control of locomotion in cat. Proc. Natl. Acad. Sci. U. S. A. *93*, 13292–13297.

Zimmer, A., Zimmer, A.M., Hohmann, A.G., Herkenham, M., and Bonner, T.I. (1999). Increased mortality, hypoactivity, and hypoalgesia in cannabinoid CB1 receptor knockout mice. Proc. Natl. Acad. Sci. U. S. A. *96*, 5780–5785.

Methods

Animals
All procedures were carried out in accordance with the European Union Directive 86/609/EEC and approved by the Champalimaud Centre for the Unknown Ethics Committee and the Portuguese Direcção Geral de Veterinária (Ref. No. 0421/000/000/2015). All procedures were performed in male and female mice approximately 10–14 weeks of age.

Global and conditional knockouts
Global CB1R knockout mice (CB1KO, CB1R -/-) (Zimmer et al., 1999) and their littermate controls (CB1R +/+) were obtained by crossing heterozygous breeding pairs (CB1R +/-). Gabra6Cre;CB1flox mice were generated by crossing mice (Gabra6Cre) in which Cre recombinase expression was driven by the promoter of the alpha6 subunit of the GABA$_A$ receptor and was specific to granule cells within the cerebellar cortex (Fünfschilling and Reichardt 2002), with mice (CB1flox, (Marsicano et al., 2003) carrying floxed alleles of the Cnr 1 gene that encodes the CB1R (Matsuda et al. 1990). The Gabra6Cre:CB1flox mouse line has been previously characterized and shown to lack parallel fiber LTD, as well as CB1R-mediated short-term forms of parallel-fiber-Purkinje cell plasticity (Carey et al., 2011). All lines were kept in a C57BL/6J background.

Surgical procedures
In all our surgeries, animals were anesthetized with isoflurane (4% induction and 0.5 – 1% for maintenance), placed in a stereotaxic frame (David Kopf Instruments, Tujunga, CA) and a custom-cut metal head plate was glued to the skull with dental cement (Super Bond – C&B). After any surgical procedure, mice were monitored and allowed ~1-2 days of recovery.

Behavioral procedures
Eyeblink conditioning
The experimental setup was based on previous work (Albergaria et al., 2018). For all behavioral experiments, mice were head-fixed but could walk freely on a Fast-Trac Activity Wheel (Bio-Serv) and habituated to the behavioral setup for at least 4 days prior to training. To externally control the speed of the treadmill, a DC motor with an encoder (Maxon) was used. For experiments on the motorized treadmill, mice were additionally habituated to walk at the target speed until they walked normally and displayed no external signs of distress. There was no difference across genotypes in the amount of habituation time.

Running speed was measured using an infra-red reflective sensor placed underneath the treadmill. Eyelid movements of the right eye were recorded using a high-speed monochromatic camera (Genie HM640, Dalsa) to monitor a 172 x 160 pixel region, at 900fps. Custom-written software using LabVIEW, together with a NI PCIE-8235 frame grabber and a NI-DAQmx board (National Instruments), was used to trigger and control all the hardware in a synchronized manner.

Acquisition sessions consisted of the presentation of 100 CS-US paired trials and 10 CS-only trials, which allow for the analysis of the kinematics of CRs without the masking effect that comes from the US-elicited reflex blink. The 110 trials were separated by a randomized inter trial interval (ITI) of 5-20s. In each trial, CS and US onsets were separated by a fixed interval (ISI) of 300ms and both stimuli co-terminated.

For all training experiments, the unconditioned stimulus (US) was an air-puff (40psi, 50ms) controlled by a Picospritzer (Parker) and delivered via a 27G needle positioned ~0.5cm away from the cornea of the right eye of the mouse. The direction of the air-puff was adjusted for each session of each mouse so that the unconditioned stimulus elicited a normal eye blink. The CS had a 350ms duration and was a white light LED positioned ~3cm directly in front of the mouse.

Eyeblink conditioning analysis
The video from each trial was analyzed offline with custom-written software using MATLAB (MathWorks). The distance between eyelids was calculated frame by frame by thresholding the grayscale image and extracting the minor axis of the ellipse that delineated the eye. Eyelid traces were normalized for each session, ranging from 1 (full blink) to 0 (eye fully open). Trials were classified as CRs if the eyelid closure reached at least 0.1 (in normalized pixel values) and occurred between 100ms after the time of CS onset and the onset of US. The average running speed for each animal was calculated by summing the average speed of each session (total distance run divided by session duration) and dividing by the total number of learning sessions, usually 20. Running speed for trial was calculated by dividing the distance run in the intertrial interval preceding the current trial by the elapsed time.

Locomotor coordination and learning
Locomotor coordination was assessed using our previously described LocoMouse setup, a tracking and analysis system for freely moving mice (Machado et al., 2015). Briefly, mice walked across a glass corridor, with

a mirror placed at 45 deg below the mouse, so that a single high-speed camera recorded both bottom and side views. Individual trials consisted of single crossings of the corridor. Mice initiated trials by walking back and forth between two dark 'home' boxes on each end of the corridor. Tracking and gait analysis was performed offline. Tracking data was first broken down into strides using a simple peak detection algorithm (Machado et al., 2015). For the analyses shown in Supp. Fig 1A, we computed a range of locomotor parameters to compare global CB1KO mice to mutants (Purkinje cell degeneration, *pcd* and reeler) with cerebellar atrophy and consequent ataxia (Lalonde and Strazielle, 2007; Mariani et al., 1977; Mullen et al., 1976). The reported gait parameters have been previously described (Machado et al., 2015). *Individual limb measures:* stride length, cadence, stance and swing duration, swing velocity. *Interlimb coordination:* double support, step length, left-right (LR) and front-hind (FH) stance phasing, % time in 1 paw, 3 paw, non-diagonal 2 paw (other) supports. *Body coordination:* front paw base of support (BOS), maximum upward motion in a stride (peak z), maximum left-right (y) of front paws (max y front paw) and nose (max y nose).

Split-belt locomotor adaptation experiments and analyses were performed on a modified version of the LocoMouse setup (Machado et al., 2015) as previously described (Darmohray et al., 2018). Two motor-driven transparent treadmill belts independently imposed the walking speed on the two sides of the body. Split-belt locomotor adaptation experiments consisted of 'baseline' tied, split-belt, and 'washout' tied belt trials. All trials were one minute in duration, with brief periods in which the motors were off, in between trials.

Granule-cell specific CB1KO mice and their littermate controls were run in a single session adaptation protocol (2 tied trials, 8 split trials; 8 tied trials). For these mice, split-belt trial speeds were at a 2.14:1 ratio: 0.175 m/s (slow) and 0.375 m/s (fast). Global CB1KO mice and their littermate controls underwent a longer, multi-session adaptation protocol consisting of 10 trials per day (session 1: 3 tied, 7 split; sessions 2-3: 10 split; session 4: 3 split, 7 tied; session 5: 10 tied), with lower overall belt speeds (tied: 0.2 m/s; slow: 0.125 m/s fast: 0.275 m/s).

For split-belt locomotor adaptation analyses (Fig. 4), we compared mutants and littermate controls on individual and interlimb coordination parameters. For individual limb analyses, we compared the two groups on their initial response to split-belt walking by assessing how stride length symmetry scaled on the first split-belt trial. To assess learning of new interlimb coordination parameters, we compared the aftereffects (first washout trial – average baseline) of mutants and littermate controls.

Histology

To confirm CB1R expression in the different mouse lines, animals were perfused transcardially with 4% paraformaldehyde and their brains removed. Sagittal sections (50um thick) were cut in a Cryostat and stained with a polyclonal guinea pig antibody raised against the last 31 amino acids of the CB1R C-terminal (from Frontier Institute co., ltd) and DAPI. Sections were mounted on glass slides with Vectashield® mounting medium and imaged with a 10x objective.

Statistical analysis

All statistical analyses were performed using the Statistics toolbox in MATLAB. For the correlation between speed and CR amplitude (Fig. 1H; Fig. 2D), we used a mixed model approach. We specified random slopes and intercepts models and included mouse/subject as a random covariate using the lme2 package (Bates, 2005). We report F tests (ANOVA) with Satterthwaite degrees of freedom correction; reported post-hoc analyses are t-tests with Tukey corrections for multiple comparisons. For the correlation between speed and onset session (Fig. 1E), we used linear regression analysis. To compare the average distance between animals of each genotype (Fig. 1D; Fig. 3C), and the average amplitudes of eyelid closure (Fig. 1I; Fig. 2D; Fig. 3G) we used a Student's unpaired t-test. We used the same test to analyze stride length in early split trials and step length aftereffect of mutants and littermate controls (Fig. 4C-F). All t-tests were two-sided. Differences were considered significant at $*p < 0.05$, $**p < 0.01$ and $***p < 0.001$. Mice were randomly assigned to specific experimental groups without bias and no animals were excluded.

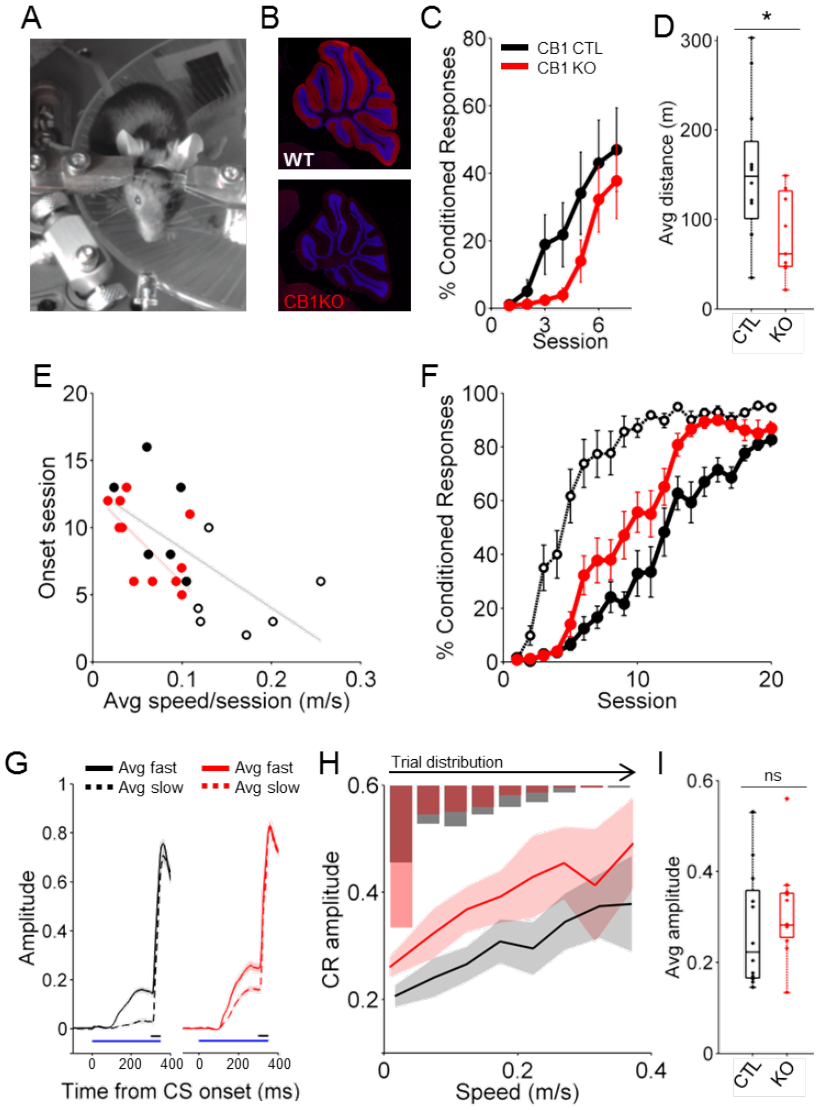

Fig. 1. Eyeblink conditioning performance correlates with locomotor activity regardless of genotype
A. Setup for eyeblink conditioning in head-fixed mice on a running wheel, showing an LED as the CS and an air puff US. **B**. Sagittal sections showing the complete elimination of CB1R (red) in CB1KOs and DAPI staining the granule cell layer (blue). Images of the cerebellum of a representative control (upper panel) and global CB1 knockout (bottom panel). **C**. Average %CR learning curves of controls (CB1 CTL, black, N=12) and global CB1 knockout mice (CB1 KO, red, N=11). Error bars indicate SEM. **D**. Average running distance of CB1 CTL (black, N=12) and CB1 KO (red, N=11) on a self-paced treadmill across 20 learning sessions. Global CB1 knockout mice were significantly hypoactive (*p = 0.015, Student's two-sided t-test). Box indicates median and 25th-75th percentiles, whiskers extend to the most extreme data points. **E**. Onset session of learning for control and CB1 KO (black and red, respectively), plotted against the animals' average walking speed. Black open circles represent CB1 CTL that ran more and their average learning curve is represented in F (dashed black line with open circles). Onset session was defined as the session in which the average CR amplitude exceeded 0.1. Each dot represents an animal. Lines are robust linear fits for all CB1 KO (red, N=11, slope = -66.5, *p = 0.02) and controls (gray, N=12, slope = -44.2, *p = 0.04). **F**. Average of %CR learning curves of CB1 KO (red line, N=11) compared with wildtype littermates with comparable average walking speed (solid black line, N=6) or with increased locomotor activity (dashed black line, N=6). Error bars indicate SEM. **G**. Average eyelid traces of slow (≤ 0.1m/s, dashed line) and fast (> 0.1m/s, solid line) trials for one representative animal of each genotype (black, controls; red, CB1KO), from the session in which that animal's learning crossed a threshold of 50% CRs, plus the following session. Blue horizontal line represents the time LED CS is on and black horizontal line represents a 50ms airpuff US. Shadows indicate SEM. **H**. Trial-to-trial correlation between CR amplitude and walking speed. Histograms indicate the relative % of trials (averaged across animals) from each genotype that fell in each speed bin. CR amplitudes for all trials from the same sessions as in (G) are plotted with lines representing averages across control (black) and global knockout (red) animals; shadows indicate SEM. There was a significant positive relationship for both controls (n=2639 trials, N=12 animals, F(1,73.7) = 35.9, ***p = 7.1e-08) and global knockouts (n=2470 trials, N=11 animals, F(1,45.5) = 62.9, ***p = 4.0e-10). **I**. Mean CR amplitudes from same sessions in (G). There was no significant difference in the average amplitude of control (black, N=12) vs. global knockout (red, N=11) animals (p = 0.44). Dots represent individual animals. Box indicates median and 25th-75th percentiles, whiskers extend to the most extreme data points.

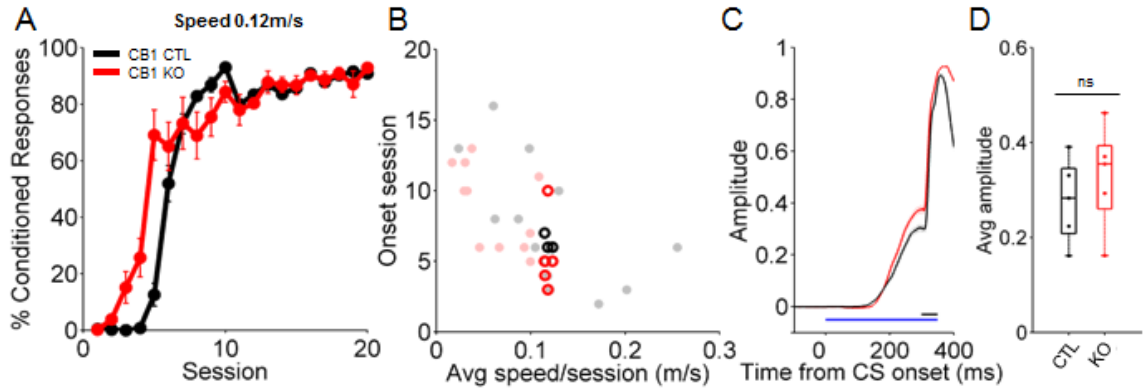

Fig. 2. Speed-dependent modulation of eyeblink conditioning on a motorized treadmill
A. Average %CR learning curves of controls (black, N=5) and global CB1 knockout (red, N=5) mice, while running at a fixed speed (0.12m/s) on a motorized treadmill. Error bars indicate SEM. **B**. Onset session of learning for control and global CB1 knockout mice (black and red, respectively) running on a motorized treadmill, superimposed on the self-paced treadmill data from Fig. 1E. **C**. Average eyelid traces of individual trials for one representative control (black) and global knockout (red) animal. Trials included from the session in which each individual animal crossed a threshold of 50% CR plus the following session. Shadows indicate SEM. **D**. Mean CR amplitudes from same sessions in (C). There was no significant difference in the average amplitude ($p = 0.45$) of CB1 CTL (black, N=5) and CB1 KO (red, N=5). Dots represent individual animals. Box indicates median and 25th-75th percentiles, whiskers extend to the most extreme data points.

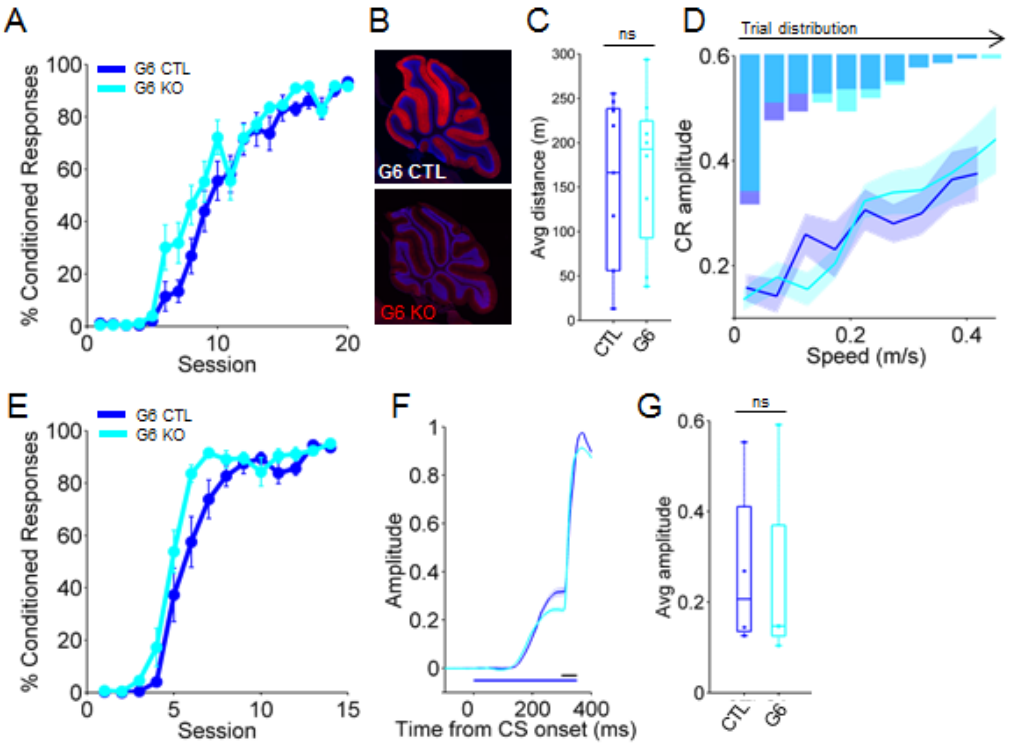

Fig. 3. Eyeblink conditioning performance is intact on granule cell-specific CB1 knockout mice
A. Average %CR learning curves of granule cell-specific CB1 knockout mice (G6 KO, cyan, N=8) and littermate controls (G6 CTL, blue, N=9). Error bars indicate SEM. **B**. Sagittal sections showing the selective elimination of CB1R (red) from cerebellar granule cells in G6 KOs and DAPI staining the granule cell layer (blue). Images of the cerebellum of a representative control (upper panel) and granule-cell conditional CB1 knockout (bottom panel). **C**. Average running distance from G6 CTL (blue, N=9) and G6 KO (cyan, N=8) mice on a self-paced treadmill across 20 learning sessions. The difference in average distance between groups was not significant. Box indicates median and 25th-75th percentiles, whiskers extend to the most extreme data points. **D**. Trial-to-trial correlation between CR amplitude and walking speed. CR amplitudes for all trials from the session in which each individual animal crossed a threshold of 50% CR plus the following session. Lines are averages across G6 CTL (blue) and G6 KO (cyan) animals; shadows indicate SEM. There was a significant positive relationship for both controls (n=1960 trials, N=9 animals, $F(1,51.1) = 20.1$, ***p = 4.2e-05) and G6 KO (n=1760 trials, N=8 animals, $F(1,47.2) = 32.6$, ***p = 7.2e-07). Histograms represent the number of trials in each bin for each group, normalized for total number of trials from the learning sessions of each animal. **E**. Average %CR learning curves of G6 KO (cyan, N=4) and G6 CTL (blue, N=4), while running at a fixed speed (0.12m/s) on a motorized treadmill. Error bars indicate SEM. **F**. Average eyelid traces of individual trials for one representative control (blue) and granule cell-selective CB1 knockout (cyan) animal. Trials included from the session in which each individual animal crossed a threshold of 50% CR plus the following session, on the motorized treadmill. Shadows indicate SEM. **G**. Mean CR amplitudes from same sessions in (E). There was no significant difference in the average amplitude (p = 0.87) of G6 CTL (blue) vs. G6 KO (cyan) animals. Dots represent individual animals. Box indicates median and 25th-75th percentiles, whiskers extend to the most extreme data points.

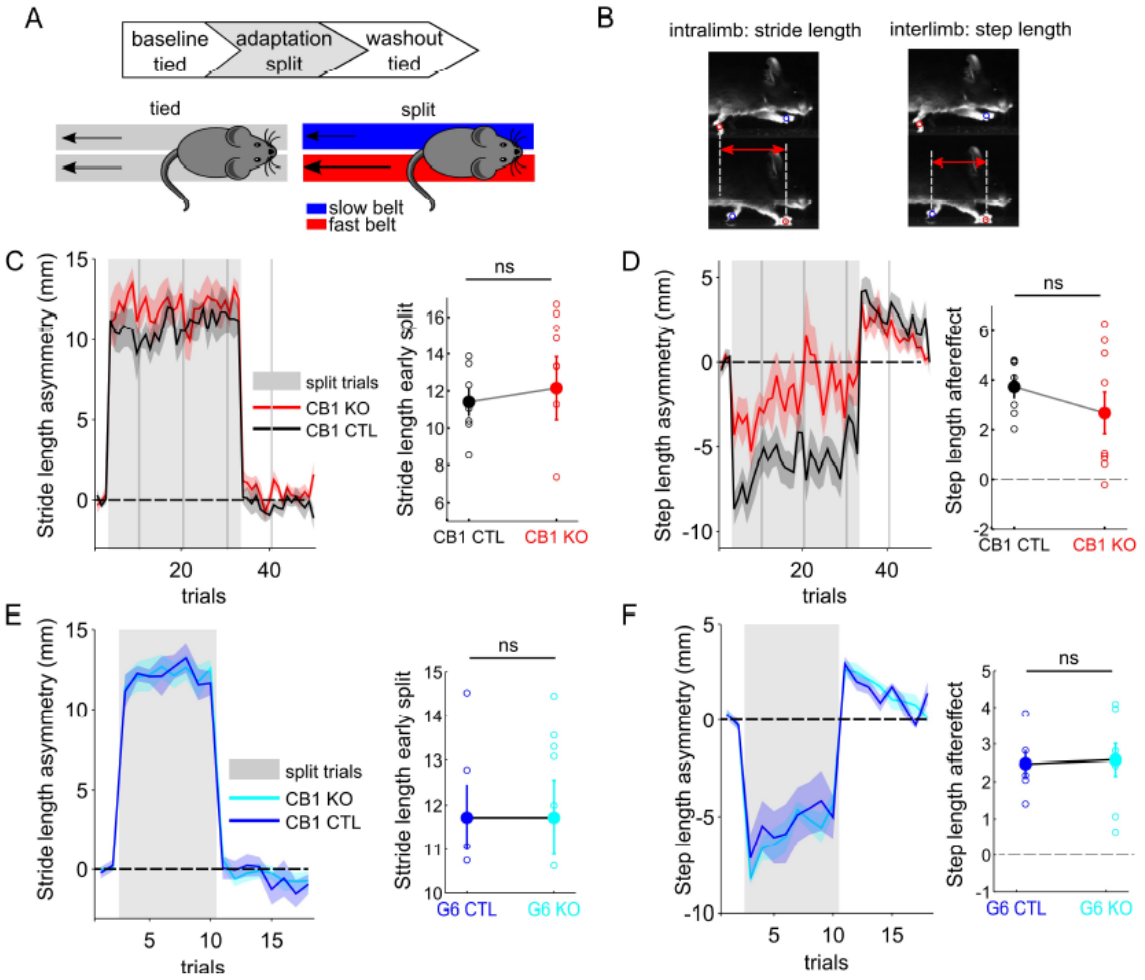

Fig. 4. Split-belt locomotor adaptation in global and granule cell specific knockout mice.
A. Experimental protocol for split-belt locomotor adaptation. Mice underwent adaptation protocols consisting of baseline, split-belt (adaptation) and washout phases. Belt speeds were equal ('tied') in baseline trials and were then abruptly split (approximately 2:1 speed ratio) for the adaptation phase, before returning to the original, symmetrical tied-belt speed in the washout phase. **B.** *Left:* The intra-limb parameter 'stride length' is the total forward motion of an individual limb from lift-off (swing) to touch-down (stance). *Right:* The interlimb parameter 'step length' is how far forward one paw is relative to its contralateral pair at stance onset. **C.** *Left:* Average front limb stride length asymmetry (fast-slow) over trials for global CB1 knockout mice (CB1 KO, n = 9, red) and littermate controls (CB1 CTL, n = 7, black). Gray shaded patch indicates split-belt trials. Vertical gray bars indicate session breaks. *Right:* Average stride length scaling (response to early split conditions) +/- SEM for CB1 global knockouts (filled circles,red) and littermate controls (filled circles, black). Individual animals are shown with smaller, open circles. **D.** L*eft:* Average front limb step length asymmetry (fast-slow) over trials for global CB1 knockout mice (CB1 KO, n = 9, red) and littermate controls (CB1 CTL, n = 7, black). Gray shaded patch indicates split-belt trials. *Right:* Average step length after-effects (first washout trial - average baseline asymmetry) +/- SEM for CB1 global knockouts (filled circles,red) and littermate controls (filled circles, black). Individual animals are shown with smaller, open circles. **E.** *Left:* Average front limb stride length asymmetry for granule cell-specific CB1 knockout mice (CB1KO, n = 8, cyan) and their littermate controls (CB1 CTL, n = 6, blue). Gray shaded patch indicates split-belt trials. *Right:* Average stride length scaling (response to early split conditions) +/- SEM for granule cell specific knockouts (filled circles,cyan) and littermate controls (filled circles, blue). Individual animals are shown with smaller, open circles. Stride length scaling: $t_{(12)} = 2.9 \times 10^{-4}$, p = 0.99 **F.** *Left:* Same as E for front limb stride length asymmetry. *Right:* Average step length after-effects +/- SEM for granule cell specific CB1 knockouts (filled circles,cyan) and littermate controls (filled circles, blue). Individual animals are shown with smaller, open circles. Step length after-effect: $t_{(12)} = -0.18$, p = 0.85.